

# Integral Equation Modelling of Reverberation Chambers using Higher-Order Basis Functions

Oscar Borries, Per Christian Hansen  
Technical University of Denmark  
Department of Applied Mathematics and Computer Science  
Kgs. Lyngby, Denmark  
*opbo@dtu.dk*

Peter Meincke, Stig B. Sørensen, Erik Jørgensen  
TICRA  
Copenhagen, Denmark  
*pme@ticra.com*

**Abstract**—Reverberation chambers (RCs) are important measurement facilities, and thus it is often required to simulate their behaviour numerically. However, due to their special characteristics, especially for high Q factors, they are often considered too challenging for application of standard numerical software. In particular, a recent publication [1] listed the perceived state-of-the-art in integral equation modelling of RCs, and identified numerous open problems.

The present paper illustrates that computational analysis of large RCs can be performed with limited computer resources. This can be achieved by using Higher-Order (HO) basis functions in the integral equation discretization and, if necessary, further applying the Multi-Level Fast Multipole Method.

After a discussion and brief review of existing methods for RC modelling, we will turn to a description of the key features of HO basis functions and their related MLFMM implementation, focusing on how they allow surpassing some of the challenges faced by lower-order discretizations. Then, several RC test cases are analyzed, drawing comparisons to other results from the relevant literature. The conclusion is that, using HO basis functions and a thorough MLFMM implementation, some of the challenges identified in [1] can be overcome.

## I. INTRODUCTION

Reverberation chambers (RCs) have seen increasing popularity over the last decade or two, and are quickly becoming a standard tool when performing Electromagnetic Compatibility tests. From the view of electromagnetics, an RC is a 3D rectangular metallic cavity with one or several mode stirrers, designed to yield a field distribution that follows the usage environment of the device under test. This includes a wide range of field strengths as well as varying polarization and directional interference.

Designing an RC which enables high-accuracy, repeatable tests that can validate a range of devices, is not trivial. The positioning and shape of the stirrer, for instance, is a subject of discussion. As the RC is designed to provide a cost-efficient testing environment, simulation of the behaviour of the RC allows its properties to be evaluated, and modified, before going to the costly construction phase.

When modelling reverberation chambers, there are in general three different approaches:

- Statistical methods, whereby statistics on the properties of the fields inside the RC are gathered.

- Full-wave, specialized algorithms. These include the Discrete Singular Convolution Method of Moments (DSC-MoM) and methods based on cavity Green's functions.
- Full-wave, general purpose algorithms. These include Finite-Difference Time Domain (FDTD), Finite Element Method (FEM) and the Method of Moments (MoM).

In general, the difficulties in finding a suitable numerical method [2] are due to the resonant characteristics of the chamber. Very fine discretizations are needed for accurate solutions, leading to convergence issues for iterative methods.

The statistical methods, sometimes combined with full-wave methods, are very useful but give only indirect information about the behaviour inside the RC.

The specialized algorithms try to avoid discretizing the chamber itself. This can be done through a layered approach [3], wherein the chamber is modelled by applying Maxwell's equations in differential form, using a 3D grid to discretize the interior of the chamber, and coupled to a MoM discretization of the stirrers and other objects inside the chamber. The drawback of this approach is a rather large use of memory, which [4] overcame at the expense of a significantly increased computational time. Note that while the chamber walls are not discretized, the interior of the chamber is, meaning that increasing the size will still lead to significantly increased computational resources.

Another specialized algorithm uses the cavity Green's functions. Here, neither the walls nor the chamber interior is discretized, which results in extreme memory reductions in the number of unknowns. [5]–[7] was limited to small wires inside the chamber due to the large overhead of evaluating the cavity Green's function. [8] significantly reduced the computational burden by employing a spectral domain factorization. Regardless, these methods cannot take into account imperfections in the chamber such as doors, slanted walls or similar effects. [2] notes that the RC door has significant impact on the solution and must be taken into account.

The general purpose algorithms can take into account a wide variety of effects, including non-rectangular chambers, arbitrarily shaped stirrers and other imperfections. However, they can have problems due to the resonant characteristics of the chamber, particularly for high Q-values. FDTD [9], [10] and the Transmission Line Matrix method (TLM) discretize

the entire interior of the chamber, yielding a very large resource consumption, particularly if accurate solutions are desired.

Finally, the Method of Moments (MoM) can discretize arbitrarily shaped chamber walls and the structures inside and is thus, in a sense, a compromise between the differential solvers and the specialised functions. Its memory requirement can still be fairly high for complex and electrically large scatterers, even when accelerated through the Multi-Level Fast Multipole Method (MLFMM).

The conclusion thus far in the literature seems to be that even for small problems, the specialized cavity Green's function approaches are the best choice, allowing for fast computations and accurate solutions. In particular, when comparing with MLFMM, cavity Green's functions are deemed to be faster and more accurate due to slow convergence of the iterative solver with MLFMM.

In the present paper, we argue that while cavity Green's function approaches have several advantages, MoM and MLFMM are useful for far larger problems than have previously been analyzed. In particular, applying Higher-Order basis functions and a suitable MLFMM implementation, large problems can be solved both rapidly and accurately, while allowing users to analyze arbitrary configurations.

## II. INTEGRAL EQUATIONS

Integral equation techniques attempt to find the surface current density induced by an incident field. Since they are based on an exact formulation, the only error sources are from the discretization and numerical solution.

Denoting the surface  $\mathcal{S}$ , the Electric Field Integral Equation (EFIE) can be expressed as

$$\mathcal{L}\mathbf{J}_S = \hat{\mathbf{n}} \times \mathbf{E}^i, \quad (1)$$

where  $\hat{\mathbf{n}}$  is a unit vector normal to  $\mathcal{S}$ ,  $\mathbf{E}^i$  is the incident electric field, and  $\mathbf{J}_S$  is the surface current density.  $\mathcal{L}$  is the integral operator

$$\mathcal{L}\mathbf{J}_S = \hat{\mathbf{n}} \times j\omega\mu \left[ \int_{\mathcal{S}} \mathbf{J}_S(\mathbf{r}') G(\mathbf{r}, \mathbf{r}') d^2\mathbf{r}' + \frac{1}{k^2} \int_{\mathcal{S}} \nabla'_S \cdot \mathbf{J}_S(\mathbf{r}') \nabla G(\mathbf{r}, \mathbf{r}') d^2\mathbf{r}' \right], \quad (2)$$

where  $\mu$  is the free-space permeability and  $k = 2\pi/\lambda$ ,  $\lambda$  being the free-space wavelength.  $G(\mathbf{r}, \mathbf{r}')$  is the free-space Green's function  $G(\mathbf{r}, \mathbf{r}') = \frac{e^{-jk|\mathbf{r}-\mathbf{r}'|}}{4\pi|\mathbf{r}-\mathbf{r}'|}$  and  $\mathbf{r}, \mathbf{r}'$  denote observation and integration points, respectively.

The Magnetic Field Integral Equation (MFIE) [11] for a smooth, closed scatterer takes the form

$$\left( \frac{1}{2}\mathcal{I} + \mathcal{K} \right) \mathbf{J}_S = \hat{\mathbf{n}} \times \mathbf{H}^i, \quad (3)$$

in which  $\mathbf{H}^i$  is the incident magnetic field,  $\mathcal{I}$  is the identity operator, and  $\mathcal{K}$  is the operator

$$\mathcal{K}\mathbf{J}_S = \hat{\mathbf{n}} \times \int_{\mathcal{S}} \mathbf{J}_S(\mathbf{r}') \times \nabla G(\mathbf{r}, \mathbf{r}') d^2\mathbf{r}', \quad (4)$$

where  $f$  denotes the Cauchy principal value and  $\hat{\mathbf{n}}$  is an outward normal unit vector. Combining EFIE and MFIE results in the Combined Field Integral Equation (CFIE) [11]

$$\left[ \alpha\mathcal{L} + (1-\alpha)\eta \left( \frac{1}{2}\mathcal{I} + \mathcal{K} \right) \right] \mathbf{J}_S = \alpha\hat{\mathbf{n}} \times \mathbf{E}^i + (1-\alpha)\eta\hat{\mathbf{n}} \times \mathbf{H}^i. \quad (5)$$

Here,  $\eta = \sqrt{\mu/\epsilon}$  is the free-space impedance,  $\epsilon$  is the free-space permittivity and  $\alpha \in [0, 1]$  is a weighting factor, usually  $\alpha = 0.5$ . The CFIE has the advantage of not having any homogenous solutions. While the MFIE and thus the CFIE is only valid for closed surfaces, it can be trivially combined with the EFIE to discretize open and closed surfaces simultaneously [12].

When discretizing the integral equation through the use of a Galerkin formulation, a linear system of the form  $\overline{\overline{\mathbf{Z}}}\overline{\overline{\mathbf{I}}} = \overline{\overline{\mathbf{V}}}$  is achieved, where  $\overline{\overline{\mathbf{Z}}}$  is an  $N \times N$  matrix. The memory requirement to store  $\overline{\overline{\mathbf{Z}}}$  is  $\mathcal{O}(N^2)$  and the solution time for a direct method is  $\mathcal{O}(N^3)$ . Therefore, it is important to reduce  $N$  as much as possible, whilst maintaining accuracy. This is most efficiently done using Higher-Order basis function on curved quadrilateral patches—we employ the Legendre basis functions [13].

### A. Acceleration of MoM

To accelerate the solution of integral equations, methods such as the Multi-Level Fast Multipole Method (MLFMM) [14]–[16] can be used. These require much less memory through a compact representation of the operator, which prohibits the use of direct methods, instead relying on an iterative solver and a preconditioner to ensure convergence of the solver.

The essential part of MLFMM is Rokhlin's translation function [14]

$$T_L(\mathbf{k}, \mathbf{x}) = \sum_{l=0}^L (-j)^l (2l+1) h_l^{(2)}(k|\mathbf{x}|) P_l(\hat{\mathbf{k}} \cdot \hat{\mathbf{x}}). \quad (6)$$

Consider two basis functions  $\mathbf{f}_j$  and  $\mathbf{f}_i$ , located in groups  $m$  and  $m'$ , respectively, that are *well-separated* such that  $|\mathbf{r}_{mm'}|$  is larger than some threshold. Given  $T_L$ , the mutual impedance between  $\mathbf{f}_j$  and  $\mathbf{f}_i$  can be expressed as

$$Z_{j,i} \simeq \kappa \iint \mathbf{R}_{jm}(\mathbf{k}) \cdot (T_L(\mathbf{k}, \mathbf{r}_{mm'}) \mathbf{V}_{im'}(\mathbf{k})) d^2\hat{\mathbf{k}}, \quad (7)$$

where  $\mathbf{r}_{xy}$  is defined as  $\mathbf{r}_{xy} = \mathbf{r}_x - \mathbf{r}_y$  and  $\mathbf{r}_m$  is the center of the group  $m$ . For EFIE,  $\kappa = -j\frac{k\eta}{4\pi}$ , while for MFIE  $\kappa = -\frac{\eta}{4\pi}$ . The accuracy of (7), when using the Excess Bandwidth Function [17] to find the truncation limit  $L$ , is directly proportional to the distance between groups  $m$  and  $m'$  and their size.

The basis function patterns  $\mathbf{V}_{jm}$  and  $\mathbf{R}_{jm}$  for EFIE are

$$\mathbf{V}_{jm}(\mathbf{k}) = \int_{\mathcal{S}} \mathbf{f}_j(\mathbf{r}) \cdot [\overline{\overline{\mathbf{I}}} - \hat{\mathbf{k}}\hat{\mathbf{k}}] e^{-j\mathbf{k} \cdot (\mathbf{r}_m - \mathbf{r})} d^2\mathbf{r}, \quad (8a)$$

$$\mathbf{R}_{jm} = \mathbf{V}_{jm}^*, \quad (8b)$$

and for MFIE

$$\mathbf{V}_{im}(\mathbf{k}) = -\hat{\mathbf{k}} \times \int_S e^{-j\mathbf{k}\cdot(\mathbf{r}_m-\mathbf{r})} [\mathbf{f}_i(\mathbf{r}) \times \hat{\mathbf{n}}(\mathbf{r})] d^2\mathbf{r}, \quad (9a)$$

$$\mathbf{R}_{im}(\mathbf{k}) = \int_S e^{-j\mathbf{k}\cdot(\mathbf{r}-\mathbf{r}_m)} \mathbf{f}_i(\mathbf{r}) d^2\mathbf{r}, \quad (9b)$$

where  $\mathbf{r}$  covers the patch on which  $\mathbf{f}_i$  is defined.

In [1], [18], the MLFMM is used to study reverberation chambers. In addition to the conclusion that the CFIE, not the EFIE, should be used for RC simulation, they conclude that MLFMM can yield very large errors when applied to RCs. These conclusions are challenged here.

### B. Choice of Integral Equation

When solving the exterior scattering problem, i.e. the scenario where a cavity with perfectly electrically conducting walls is illuminated by an outside field, both the EFIE and the MFIE suffer from the presence of homogeneous solutions inside the closed cavity, whereas the CFIE provides a unique solution at all frequencies. In particular, the homogeneous solutions for the MFIE inside the cavity actually radiate a field outside it, which makes the MFIE a very poor choice for such problems.

When solving the interior cavity problem, where the source is placed inside the cavity — as is the case for the RC problems considered in the present paper — all three integral equations can be used since no homogeneous solution can exist in the exterior region extending to infinity. Thus, the only difference between the three formulations is the condition number of the resulting matrix. Since MFIE results in the lowest condition number, the MFIE is the best formulation for solving the interior cavity problem. We note that for such interior problems, the normal vector in (4) and (5) is directed into the cavity.

### C. MLFMM and Reverberation Chambers

When applying the MLFMM, the expansion of the Greens function around a center ( $\mathbf{r}_m$  in (8)) is translated by the translation function  $T_L$ . The accuracy of the expansion depends on the diameter of the groups and the distance  $|\mathbf{r}_m - \mathbf{r}_{m'}|$  between the groups. Assuming that the diameter of the groups is  $D$  such that the side length of the groups is  $a = D/\sqrt{3}$ , the minimum distance for which (7) is applied is  $|\mathbf{r}_m - \mathbf{r}_{m'}| = 2a$ . At this short distance, the error in the expansion can be significantly larger than the theoretical estimates predict [19], particularly for small groups. Figure 1 illustrates the scenario.

Usually, this is not in itself a significant problem, because it might not affect the radiated field much. However, for cavities such as a reverberation chamber, the effects of the resonant nature of the chamber are so severe that the aforementioned errors are very apparent in the solution [1]. The only viable way to avoid this is to increase the size of the groups, but this results in a significant increase in memory.

However, for MLFMM based on Higher-Order (HO) basis functions, the groups are already significantly larger than for RWG based solutions, and therefore MLFMM based on HO (HO MLFMM) basis functions allows for much better

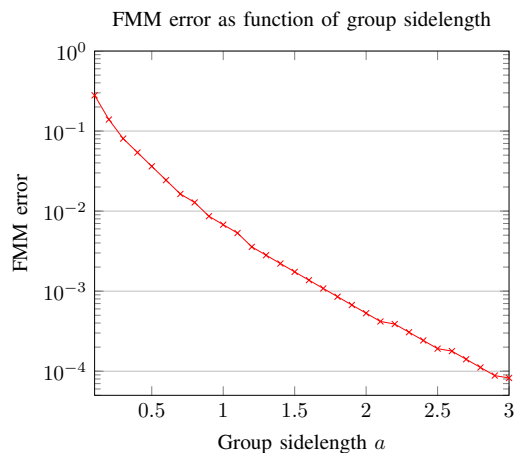


Fig. 1: The relative error between FMM and MoM as a function of group size for two groups separated by the minimum distance at which the FMM is applicable,  $2a$ .

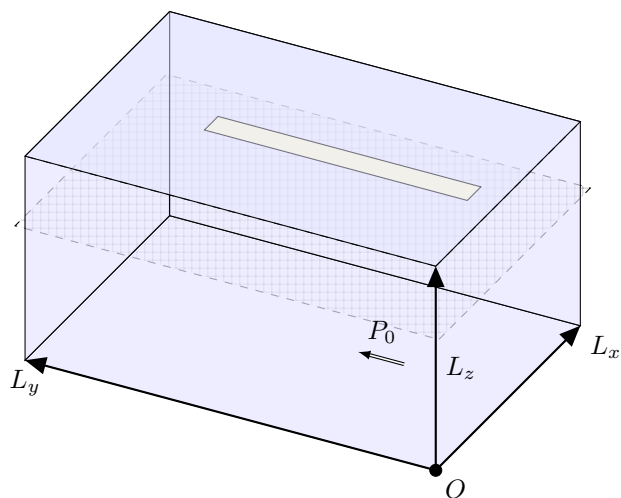


Fig. 2: The geometry for test case A. The white stirrer is positioned at the top of the chamber, and the dashed plane, which extends slightly beyond the chamber walls, indicates the plane on which we compute the field.

error control than MLFMM based on Lower-Order (LO) basis functions. Further, HO MLFMM was shown in [20] to be more efficient than LO MLFMM, even when the groups are as small as possible. Thus, when LO MLFMM is applied to RC problems, requiring oversized groups, HO MLFMM is even more advantageous relative to LO MLFMM.

## III. NUMERICAL RESULTS

In this section, we will consider some test cases, drawing comparisons to results available in the literature. Comparing the memory is straight-forward, and since the results from the literature are fairly recent, we can to some extent also compare the computational time spent.

### A. Simple Chamber with Stirrer

We will begin by considering a geometry studied in [1], [3], [4], a fairly large reverberation chamber with a single, flat plate as a stirrer. The configuration is illustrated in Figure 2, and the relevant parameters are given in Table I. As a source, we use a  $\hat{y}$ -directed point source at  $(p_x, p_y, p_z)$ . We evaluate the field on a plane at  $z = 4$  m, extending beyond the chamber walls, allowing us to inspect whether the field is actually zero (as it should be) outside the chamber.

TABLE I: Configuration parameters, test cases A and B.

Symbol	Parameter	Case A	Case B
$L_x$	Chamber size along $\hat{x}$	8.5 m	8 m
$L_y$	Chamber size along $\hat{y}$	12.5 m	4.5 m
$L_z$	Chamber size along $\hat{z}$	6 m	2.8 m
$S_x, S_y$	Stirrer dimensions	0.8 m, 8 m	3.6 m, 1.2 m
$p_x, p_y, p_z$	Position of source	(2, 2, 1.6) m	(2, 2, 1.6) m

The computational requirements are shown in Table II and compared to similar results from previous publications. Our runtimes are from a modern laptop, 2.6 GHz Intel i7, while the other publications used an unspecified 2.67 GHz CPU, meaning that we can roughly compare the computational runtimes. For the lower frequency  $f = 82$  MHz, the problem is so small that an iterative solver is not necessary when using Higher-Order basis functions—using patches with  $2\lambda$  sidelength with up to 9<sup>th</sup> order basis functions, we use 886 unknowns, meaning that a direct factorization of the  $\bar{\bar{Z}}$  matrix is by far the fastest solution. We use 2.4 seconds and 6 MB of memory, which is 1-2 orders of magnitude less than that reported in [1], [3], [4] for MoM and MLFMM as well as a specialized, hybrid approach (DSC).

Increasing the frequency to  $f = 200$  MHz means that the number of unknowns is increased by roughly a factor of 6. For the RWG basis functions used by [1], [3], [4], this results in a high number of unknowns. In turn, this means that their direct MoM solution requires 30 GB memory and thus is not an appealing alternative for standard workstations. Turning to MLFMM, the use of RWG basis functions and thus small groups results in high error levels, as discussed in Section II-C, and long runtimes, while their use of CFIE results in slower convergence. In contrast, for HO basis functions, only 5162 unknowns are necessary, resulting in 0.2 GB of memory, meaning that a direct solution is well within the capabilities of most computers. Further, if an iterative solution using MLFMM is desired, the use of HO basis functions and the MFIE results in a short solution time and low relative error.

As a further confirmation of the applicability of MFIE for this problem, Figure 3 compares the error achieved by MFIE and EFIE relative to the solution achieved with CFIE. The Figure clearly illustrates that the error patterns are similar, suggesting that MFIE is at least as accurate as EFIE, but converges much faster.

### B. Larger Chamber

As a second test case, we consider another chamber, taken from [8]. The general layout of the chamber is similar to

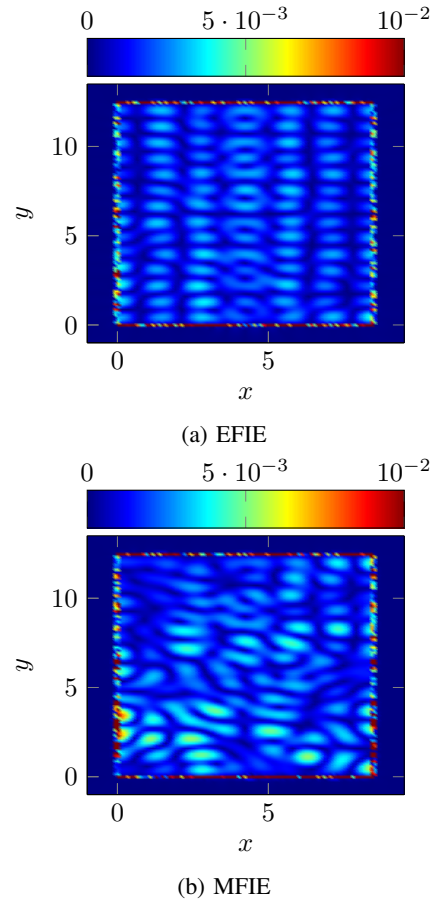


Fig. 3: The error, relative to the solution achieved by CFIE, when applying EFIE and MFIE, respectively. The very rapidly varying error occurs at the walls of the RC.

testcase A, although the room is electrically slightly larger. The exact dimensions are as given in Table I, where we note that we use a dipole as a source, located in the same position as test case A.

We again apply the MFIE and our Higher-Order MoM code to solve the problem, and achieve the computational times given in Table III.

We compare our computational loads with that of the cavity Green’s function (CGF) code from [8], which also posted results from a reference MLFMM implementation based on low order basis functions. We consider the room at three separate frequencies, and note that while our Higher-Order MoM code uses much fewer unknowns than their low order MLFMM, it still uses more unknowns than their CGF implementation. However, the runtimes using CGF are an order of magnitude higher than for our Higher-Order implementation.

While the number of unknowns is larger using Higher-Order MoM, since MoM discretizes the entire structure while the CGF only needs to discretize the stirrer, the problems considered here are far from memory limited on a modern computer and allow the use of a direct solver. Therefore, the primary performance parameter is expected to be the time consumption.

TABLE II: Computational results from test case A. The error is relative to that achieved by the direct MoM solution. Greyed out boxes indicate non-applicable information, while blacked out boxes indicate unavailable information. Total time includes both setup time and solver time.

$f=82$ MHz	Results from [1], [3], [4]			Our code	
	MoM	MLFMM	DSC	MoM	MLFMM
No. unknowns	11239		3915		886
No. iterations	$\approx 250$			Direct	
Relative error		0.068-0.017			
Time pr it. [s]	3.85	1.34-1.26			
Total time [s]	$\approx 960$	$\approx 325$	183-887	2.4	
Memory [MB]	973	47-126	31-675	6	
$f=200$ MHz	MoM	MLFMM	DSC	MoM	MLFMM
No. unknowns	63,480				5162
No. iterations	$\approx 2000$			Direct	347
Relative error		$> 10^{-2}$			$2 \cdot 10^{-3}$
Time pr it. [s]		$\approx 10$			0.17
Total time [s]		$\approx 20,000$		13.1	89
Memory [GB]	30	0.63		0.2	0.15

TABLE III: Results from test case B.

$f=100$ MHz	Results from [8]		Our code	
	Cavity	MLFMM	MoM	MLFMM
Unknowns	147	4935		512
Total time [s]	3.4	45	0.28	
$f=200$ MHz	Cavity	MLFMM	MoM	MLFMM
Unknowns	569	19847		1668
Total time [s]	21.5	1110	1.9	
$f=400$ MHz	Cavity	MLFMM	MoM	MLFMM
Unknowns	2292	78306		5760
Total time [s]	517.3	11774	18.5	107

### C. Chamber with Door

The previous examples highlighted the memory and speed advantages of Higher-Order MoM, as well as the accuracy advantage of HO-MLFMM, even when compared against specialized RC codes.

However, an important consideration when modelling RCs are that the chamber is, in fact, far from a perfect rectangular cavity. Elements such as the door and the mounting of the device-under-test are very important for the scattered field due to the resonant nature of the chamber [2]. The specialized codes considered previously are significantly less effective when the mounting structures have to be included, and codes based on cavity Green's function cannot take the door or other wall imperfections into account. Furthermore, some RCs are designed with slanted, moveable walls, such that the walls themselves can act as mode stirrers.

To demonstrate the general applicability of our approach, and confirm previous findings in the literature concerning the effect of including the RC door, we slightly modify test case A to include a door. The door is 2 m high, 1 m wide and 0.1 m deep, and is shown together with the rest of the chamber in Figure 4. We calculate the behaviour at  $f = 200$  MHz, where we note that the door is roughly  $0.07\lambda$  deep, so electrically speaking, the test case is not far from a perfect rectangular chamber.

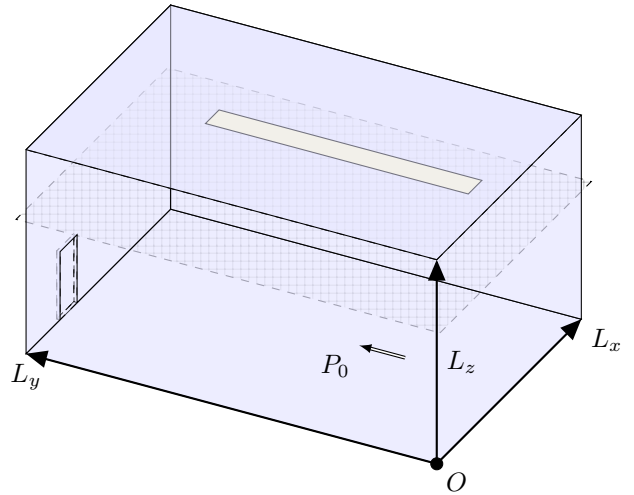


Fig. 4: Reverberation chamber with a door, for test case C.

The  $\hat{z}$ -component of the electric field is shown in Figure 5, both with and without door. Clearly, the effects of the electrically small door cannot be ignored, and thus methods based on cavity Green's function will have some issues when applied to realistic chambers.

The number of unknowns needed for our simulation is 6170, slightly more than we used in test case A for the perfect rectangular chamber, where we needed 5162. This is not only due to the door, but also because we need a finer mesh of the chamber walls when including the door, to ensure connectivity of the mesh. While this yields a slightly larger memory consumption, a direct solution is still feasible. Had we used RWG basis functions, the problem would have required roughly 25000 unknowns, in which case a direct solution would require much more time due to the  $N^3$  scaling of the solution time of a direct solver.

## IV. CONCLUSION

We have considered several different reverberation chambers, comparing our Higher-Order Method of Moments code to results from the literature. In general, both with regards to speed and memory, Higher-Order MoM is by far the best approach of those considered. Methods based on cavity Green's function are less memory demanding but significantly slower and only relevant for extremely large problems where memory consumption is the limiting factor. Further, they cannot be applied for realistic chambers that include doors and other imperfections.

Also, we have shown that the MFIE is a better integral equation than EFIE and CFIE for RC modelling, since the lack of homogenous solutions allows us to exploit the well-conditioning of the MFIE. Thus, the general purpose HO-MoM and, if needed due to memory, HO MLFMM, applied to the MFIE is the best method for analyzing realistic chambers.

## REFERENCES

- [1] H. Zhao, "MLFMM-Accelerated Integral-Equation Modeling of Reverberation Chambers," *IEEE Antennas and Propagation Magazine*, vol. 55, no. 5, pp. 299–307, Oct. 2013.
- [2] C. Bruns and R. Vahldieck, "A closer look at reverberation Chambers - 3-D Simulation and experimental verification," *IEEE Transactions on Electromagnetic Compatibility*, vol. 47, no. 3, pp. 612–626, 2005.
- [3] H. Zhao and Z. Shen, "Efficient Modeling of Three-Dimensional Reverberation Chambers Using Hybrid Discrete Singular Convolution-Method of Moments," *IEEE Transactions on Antennas and Propagation*, vol. 59, no. 8, pp. 2943–2953, 2011.
- [4] —, "Memory-Efficient Modeling of Reverberation Chambers Using Hybrid Recursive Update Discrete Singular Convolution-Method of Moments," *IEEE Transactions on Antennas and Propagation*, vol. 60, no. 6, pp. 2781–2789, Jun. 2012.
- [5] F. Gronwald, "Calculation of mutual antenna coupling within rectangular enclosures," *IEEE Transactions on Electromagnetic Compatibility*, vol. 47, no. 4, pp. 1021–1025, 2005.
- [6] U. Carlberg, P. S. Kildal, and J. Carlsson, "Study of antennas in reverberation chamber using method of moments with cavity Green's function calculated by Ewald summation," *IEEE Transactions on Electromagnetic Compatibility*, vol. 47, no. 4, pp. 805–814, 2005.
- [7] K. Karlsson, J. Carlsson, and P. S. Kildal, "Reverberation Chamber for Antenna Measurements: Modeling Using Method of Moments, Spectral Domain Techniques, and Asymptote Extraction," *IEEE Transactions on Antennas and Propagation*, vol. 54, no. 11, pp. 3106–3113, 2006.
- [8] M. E. Gruber and T. F. Eibert, "Simulation of reverberation chambers using method of moments with cavity Green's function and spectral domain factorization," *Electromagnetic Compatibility (EMC), 2013 IEEE International Symposium on*, pp. 808–812, 2013.
- [9] F. Moglie, "Convergence of the reverberation chambers to the equilibrium analyzed with the finite-difference time-domain algorithm," *IEEE Transactions on Electromagnetic Compatibility*, vol. 46, no. 3, pp. 469–476, 2004.
- [10] F. Moglie and V. M. Primiani, "Reverberation chambers: Full 3D FDTD simulations and measurements of independent positions of the stirrers," *Electromagnetic Compatibility (EMC), 2011 IEEE International Symposium on*, pp. 226–230, 2011.
- [11] J. R. Mautz and R. F. Harrington, "H-Field, E-Field, and Combined Field Solutions for Bodies of Revolution," *Syracuse University, Department of Electrical and Computer Engineering*, Mar. 1977.
- [12] Ö. Ergül and L. Gürel, "Iterative Solutions of Hybrid Integral Equations for Coexisting Open and Closed Surfaces," *IEEE Transactions on Antennas and Propagation*, vol. 57, no. 6, pp. 1751–1758, 2009.
- [13] E. Jørgensen, J. Volakis, P. Meincke, and O. Breinbjerg, "Higher Order Hierarchical Legendre Basis Functions for Electromagnetic Modeling," *IEEE Transactions on Antennas and Propagation*, vol. 52, no. 11, pp. 2985–2995, Nov. 2004.
- [14] V. Rokhlin, "Diagonal Forms of Translation Operators for Helmholtz Equation in Three Dimensions," *Yale University, Tech. Rep.*, 1992.
- [15] C.-C. Lu and W. C. Chew, "A Multilevel Algorithm for Solving a Boundary Integral Equation of Wave Scattering," *Microwave and Optical Technology Letters*, vol. 7, no. 10, Jul. 1994.
- [16] J. M. Song and W. C. Chew, "Multilevel fast-multipole algorithm for solving combined field integral equations of electromagnetic scattering," *Microwave and Optical Technology Letters*, vol. 10, no. 1, pp. 14–19, Sep. 1995.
- [17] J. Song and W. C. Chew, "Error Analysis for the Truncation of Multipole Expansion of Vector Green's Functions," *IEEE Microwave and Wireless Components Letters*, vol. 11, no. 7, pp. 311–313, Jul. 2001.
- [18] H. Zhao, E. Li, and Z. Shen, "Modeling of reverberation chamber using FMM-Accelerated hybrid integral equation," in *Antennas and Propagation (APCAP), 2012 IEEE Asia-Pacific Conference on*, 2012, pp. 213–214.
- [19] M. L. Hastriter, S. Ohnuki, and W. C. Chew, "Error control of the translation operator in 3D MLFMA," *Microwave and Optical Technology Letters*, vol. 37, no. 3, pp. 184–188, May 2003.
- [20] O. Borries, P. Meincke, E. Jørgensen, and P. C. Hansen, "Multi-level Fast Multipole Method for Higher-Order Discretizations," *Accepted by IEEE Transactions on Antennas and Propagation*, 2013.

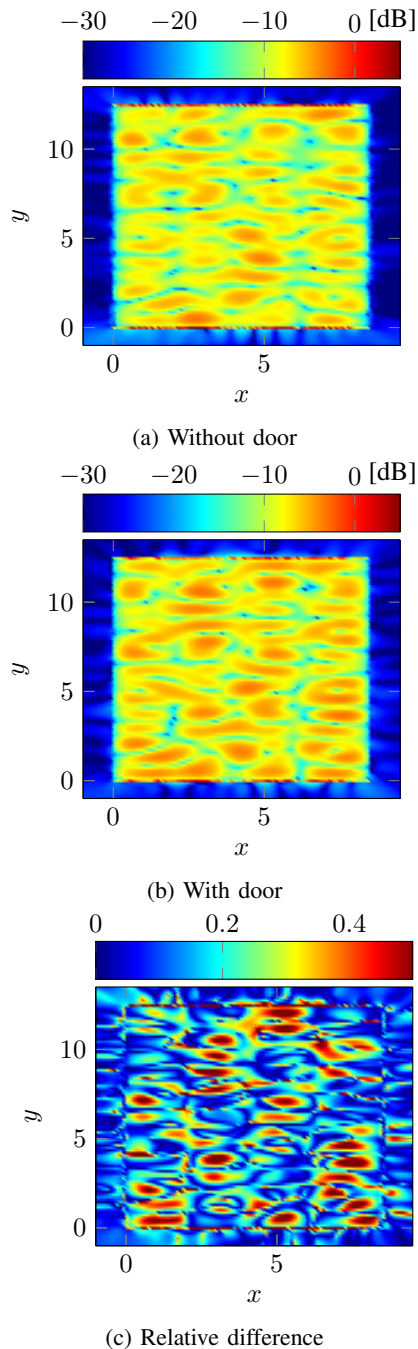


Fig. 5: The  $\hat{z}$  component of the electric field, without and with a small door. Also shown is the relative difference between the two results.